CuO-Modified PtSe$_2$ Monolayer as a Promising Sensing Candidate toward C$_2$H$_2$ and C$_2$H$_4$ in Oil-Immersed Transformers: A Density Functional Theory Study

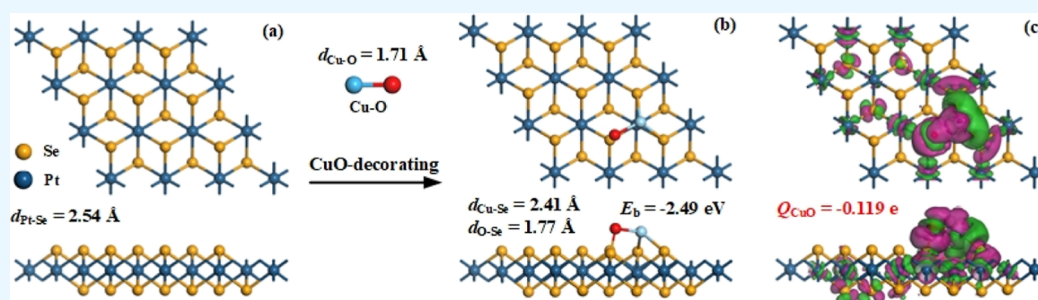Longzhen Wang, Jianfang Chen,* Changhong Liu, Min Wei, and Xuchu Xu

Read Online

ACCESS | Metrics & More | Article Recommendations

ABSTRACT: This work using the density functional theory simulates the strong potential of the CuO-decorated PtSe$_2$ (CuO−PtSe$_2$) monolayer as a recycle use C$_2$H$_2$ and C$_2$H$_4$ sensor in order to realize the arc discharge monitoring based on the nano-sensing method. Results indicate that CuO decoration causes strong n-type doping for the PtSe$_2$ monolayer with a binding force (E_b) of −2.49 eV, and the CuO−PtSe$_2$ monolayer exhibits strong chemisorption and electron-accepting properties in the two gas systems, with the adsorption energy (E_{ad}) and charge transfer (Q_T) obtained as −1.19 eV and 0.040 e for the C$_2$H$_2$ system and as −1.24 eV and 0.011 e for the C$_2$H$_4$ system, respectively. The density of states reveals the deformed electronic property of the CuO−PtSe$_2$ monolayer in gas adsorptions, and its sensing mechanism based on the change of electrical conductivity and the work function are uncovered. This work sheds light on the metal-oxide-decorated transition-metal dichalcogenides for gas sensor applications and would provide the guidance to explore novel sensing materials in many other fields as well.

1. INTRODUCTION

In the power system, electrical transformers play a significant role in carrying out the electricity conversion and transmission, and the oil-immersed transformers account for 90%.[1] In an oil-immersed transformer, the mineral oil is employed as the insulation medium to prevent the possible insulation defects.[2] For example, the temperature inside the oil would be inevitably increased after a long-term running, causing partial over-heating, and the existence of rags inside the oil can cause partial discharge. These insulation defects would release a large amount of energy and discompose the oil inside the transformers,[3,4] forming many hydrocarbons such as C$_2$H$_2$ and C$_2$H$_4$, which accounts for the dominant content of the dissolved gas species in the oil when arc discharge occurs.[5,6] Many reports have proved that these gas species have a remarkable adverse impact on the insulating performance of the mineral oil, posing a potential threat to the safe operation of such electrical equipment.[7,8] Therefore, the experts and scholars have put forward dissolved gas analysis (DGA) to evaluate the operation conduction of the oil-immersed transformers through the detections of the gases in the oil,[9,10] which nowadays has been regarded as a workable and efficient manner to that end.[11,12]

To realize the DGA, the gas detection is of great importance, which should have the advantage of high sensitivity, rapid response, and low cost.[13] Recently, the two-dimensional transition-metal dichalcogenides (TMDs), namely, monolayer TMDs, are demonstrated as novel sensing materials for the detection of gas species[14−16] due to their desirable and tunable semiconducting property in line with the strong chemical reactivity toward gas molecules.[17,18] Besides, the noble TMDs, formed by the novel metal atomic layer sandwiched by two chalcogen atomic layers, are theoretically explored for gas sensing application as well.[19,20] For example, the PtSe$_2$ monolayer has been reported to have good sensitivity and
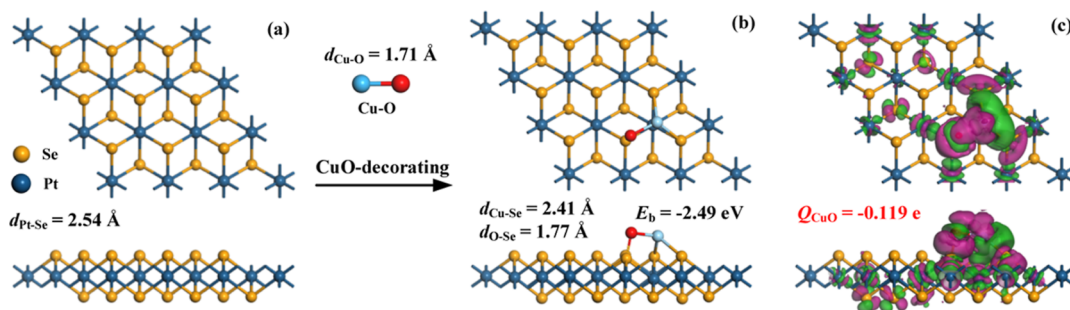
Figure 1. CuO-decorating process on the pristine PtSe$_2$ monolayer. (a) Pure PtSe$_2$ monolayer. (b,c) Morphology and CDD of CuO–PtSe$_2$. In the CDD, the green and rosy areas are electron accumulation and electron depletion, respectively, and the isosurface is set to be 0.01 eV/A^3.

rapid sensing performance as a gas sensor.[21] Besides, the metal-doped PtSe$_2$ monolayer is theoretically investigated with much stronger adsorption and sensing behaviors toward gaseous species in comparison with the pristine counterpart.[22,23] Moreover, for surface decoration to enhance the adsorption performance of the nano-surface, metal oxide medication is also accepted as a useful method.[24] For instance, the CuO- and NiO-decorated SnS$_2$ monolayer is reported with remarkably enhanced binding energy and charge transfer for gas adsorptions than the pristine SnS$_2$ surface.[25] However, to the best of our knowledge, there have been few reports about the metal-oxide-modified PtSe$_2$ monolayer as a novel gas sensing material, which needs to be investigated thoroughly for elucidating the possibility to explore such a kind of novel sensing candidate for gas detections.

In this work, we propose the CuO-decorated PtSe$_2$ (CuO–PtSe$_2$) monolayer as a potential sensing material for detections of C$_2$H$_2$ and C$_2$H$_4$ in the transformer oil, using the density functional theory (DFT). One can assume that the CuO nanoparticle could largely enhance the adsorption performance of the PtSe$_2$ monolayer given the desirable catalytic property of the Cu atom[26] as well as the existence of the O atom, which can promote the charge transfer in surface interactions.[27] It should be mentioned that a CuO nanoparticle is adsorbed on the pristine PtSe$_2$ monolayer to establish the CuO–PtSe$_2$ morphology and to analyze its adsorption and sensing mechanisms upon two gas species. We aim at uncovering the potential of such a novel material as a C$_2$H$_2$ and C$_2$H$_4$ sensor in order to evaluate the operation status, especially the arc discharge, of the oil-immersed transformers. It is our hope that our theoretical calculations can raise the attentions toward the metal-oxide-decorated PtSe$_2$ monolayer for its use in many other fields and not limited to gas detections.

2. COMPUTATIONAL METHODS

The whole DFT calculations in this report were implemented in the DMol^3 package,[28] in which we selected the generalized gradient approximation and the Perdew–Burke–Ernzerhof (PBE) functional to deal with the electron correlations and exchange.[29] Within the Brillouin zone, the k-point was sampled as $10 \times 10 \times 1$ for both geometric and electronic calculations.[30] The dispersion-corrected DFT-D2 method, proposed by Tkatchenko and Scheffler, was employed to address the van der Waals force and long-term reaction.[31] The global orbital cutoff radius of 5.0 Å along with the energy tolerance accuracy of 10^{-5} Ha was selected to ensure the good accuracy of the results of the established configurations.[32]

A $4 \times 4 \times 1$ supercell is established for the PtSe$_2$ monolayer, with a vacuum layer of 20 Å to prevent the interface

interactions between adjacent units.[33] We adopted the Hirshfeld population method to analyze the charge of the CuO nanoparticle (Q_{CuO}) in the surface decoration and the charge transfer (Q_T) in the gas adsorption systems, and the positive value indicates the electron-donating property of the CuO nanoparticle or the gas species.[33]

3. RESULTS AND DISCUSSION

3.1. Pristine PtSe$_2$ Monolayer and Surface Decoration by CuO.
The CuO–PtSe$_2$ monolayer in the current study is established by adsorption of a CuO nanoparticle on the surface of a pristine PtSe$_2$ monolayer; therefore, the decorating concentration can be calculated to be 6.9% from the atomic aspect. In the meanwhile, the geometric and electronic properties of the most stable configuration (MSC) of the CuO–PtSe$_2$ monolayer are supposed to be compared with those of the pristine counterpart. The CuO-decorating process is seen in Figure 1, in which the d means the bond length and the binding force (E_b) means the binding force between the CuO nanoparticle and the PtSe$_2$ surface, calculated using[34]

$$E_b = E_{Cu–PtSe_2} - E_{PtSe_2} - E_{CuO} \tag{1}$$

where $E_{CuO–PtSe_2}$ and E_{PtTe_2} are the total energies of CuO–PtTe$_2$ and pristine PtTe$_2$, respectively. Besides, the charge density difference (CDD) is plotted in Figure 1 as well to help observe the charge distribution of the CuO–PtSe$_2$ monolayer. One should note that the CDD here is plotted using the total electron density of the CuO–PtSe$_2$ monolayer subtracting the electron densities of the isolated CuO and the pristine PtSe$_2$ monolayer.

For the pristine PtSe$_2$ monolayer, the Pt–Se bond length is measured to be 2.54 Å and the constant lattice is obtained as 3.72 Å, which are in good accordance with the previous ref 35. The Cu–O bond length of the CuO nanoparticle is measured to be 1.71 Å. In terms of the preferred CuO–PtSe$_2$ configuration, it is seen that the CuO nanoparticle is basically parallel with the PtSe$_2$ surface, and the Cu atom is captured by two Se atoms, while the O atom is captured with the other Se atom (all three Se atoms at the upper atomic layer are bonded with the Pt atom). The Cu–Se and O–Se bond lengths are measured to be 2.41 and 1.77 Å, respectively, which are quite close to the sum of covalent radii of the Cu and Se atoms (2.28 Å) or the O and Se atoms (1.79 Å), suggesting the strong binding force between them. Through the definition of E_b, the E_b for CuO adsorption on the PtSe$_2$ monolayer is calculated to be −2.49 eV, which reveals the exothermicity and spontaneity of the CuO decoration process.
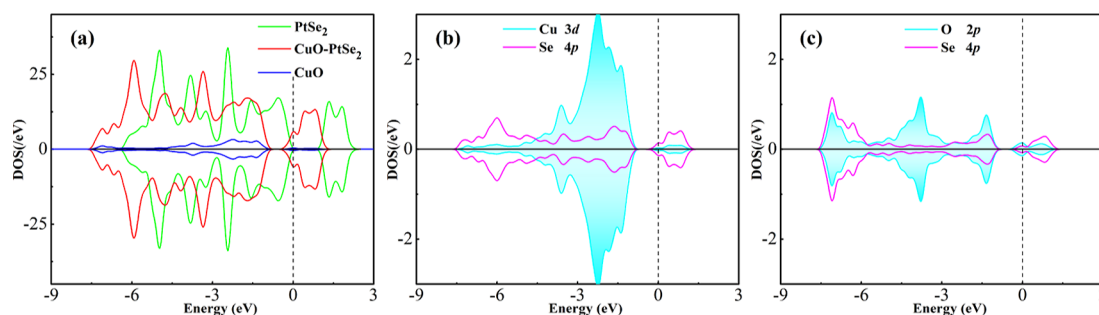
Figure 2. DOS distributions of (a) total DOS of pristine and CuO-decorated PtSe$_2$ monolayers, (b) orbital DOS of Cu and Se atoms, and (c) orbital DOS of O and Se atoms. The dashed line is the Fermi level, and the smearing is 0.1 eV.
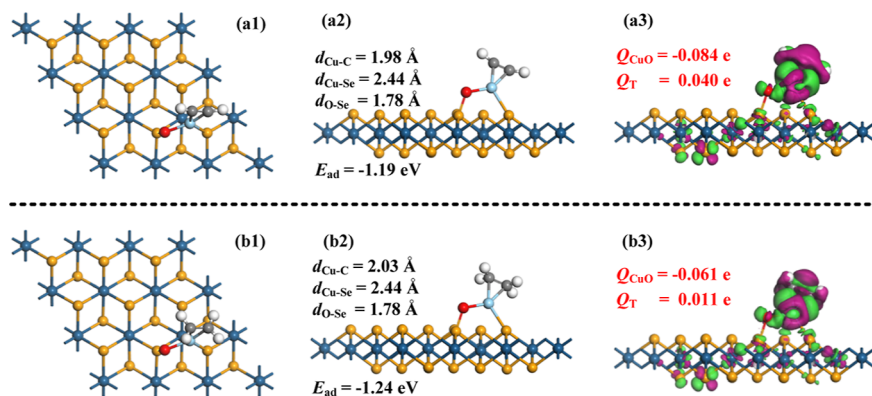

Figure 3. MSC and CDD for (a1–a3) C$_2$H$_2$ and (b1–b3) C$_2$H$_4$ adsorption on the CuO−PtSe$_2$ monolayer. In the CDD, the set is equivalent to that in Figure 1.

From the CDD configuration, one can observe that the electron accumulations are mainly distributed on the O atom of the CuO nanoparticle and the Cu−Se bond, while the electron depletions are mainly distributed on the Cu atom, the O−Se bond, and the Cu−O bond. These findings manifest the electron-accepting property of the O atoms and the orbital hybridization on the Cu−Se bonds, which reveals their strong binding force, and the electron-donating property of the Cu atom and the weakened binding force of the O−Se and Cu−O bonds. In fact, the prolonged bond length of Cu−O measured to be 1.99 Å suggests its weaker binding force in comparison with that in the isolated CuO nanoparticle as well. Besides, the Hirshfeld analysis can further support the CDD distributions. It is found that the CuO nanoparticle is charged by −0.119 e, manifesting its electron-accepting property as a whole, in which the Cu and O atoms are, respectively, charged by 0.192 and −0.311 e. Two Se atoms bonded with the Cu atom are negatively charged by 0.060 and 0.065 e, which compared with the charged value of Se atoms (−0.047 e) in the pristine PtSe$_2$ monolayer indicates their electron-accepting property. In the meanwhile, the Se atom bonded with the O atom is charged by 0.152 e, which shows its electron-donating property. These charge transfer performances may be related to the electronegativity among the Cu, O, and Se atoms, which are in the order of O (3.44) > Se (2.55) > Cu (1.90).[36]

Figure 2 depicts the density of states (DOS) of the pristine and CuO-decorated PtSe$_2$ systems, as well as the orbital DOS, to illustrate the modified electronic property of the PtSe$_2$ monolayer by CuO adsorption. From the total DOS, the pristine PtSe$_2$ monolayer exhibits a semiconducting property with the band gap of 1.31 eV, which agrees with the previous report using the PBE functional;[22] in the meanwhile, the DOS

of the CuO−PtSe$_2$ monolayer is remarkably left-shifted in comparison with that of the pristine PtSe$_2$ monolayer, and a novel peak is observed, within the bottom of the conduction band, standing at the Fermi level. Also, the band gap of the CuO−PtSe$_2$ monolayer is calculated to be 0.00 eV. These findings manifest the strong n-type doping for the PtSe$_2$ monolayer after the adsorption of the CuO nanoparticle,[37] enabling the CuO−PtSe$_2$ system to exhibit a metallic property accordingly.[38] Besides, the CuO nanoparticle contributes largely to the total DOS of the CuO−PtSe$_2$ monolayer, namely, at −7.1, −4.7 to −0.9 and 0.0 (Fermi level) eV. From the orbital DOS, one can see that the Cu 3d orbital is hybridized with the Se 4p orbital at −7.3 to −0.8 and −0.2−1.2 eV, and the O 2p orbital is hybridized with the Se 4p orbital at −7.6−0.9 and −0.4−1.2 eV. These DOS state hybridizations reveals the strong orbital interactions between Cu and Se atoms and O and Se atoms[39] during the formation the Cu−Se and O−Se bonds, respectively.

3.2. Adsorption Performances of CuO–PtSe$_2$ upon Gas Species. Above the CuO nanoparticle of the CuO−PtSe$_2$ monolayer, the adsorptions of C$_2$H$_2$ and C$_2$H$_4$ are implemented through various configurations to identify the MSC of the gas adsorbed systems. The adsorption energy (E_{ad}) is defined to evaluate the binding strength between the CuO−PtSe$_2$ monolayer and the gas species and to identify the MSC (the configuration with the most negative E_{ad}), calculated using[40]

$$E_{ad} = E_{CuO-PtSe_2/gas} - E_{CuO-PtSe_2} - E_{gas} \qquad (2)$$

wherein $E_{CuO-PtSe_2/gas}$ and E_{gas} represent the energies of the adsorbed system and freestanding gas molecule, respectively. After geometric relaxations, the MSC and related CDD for
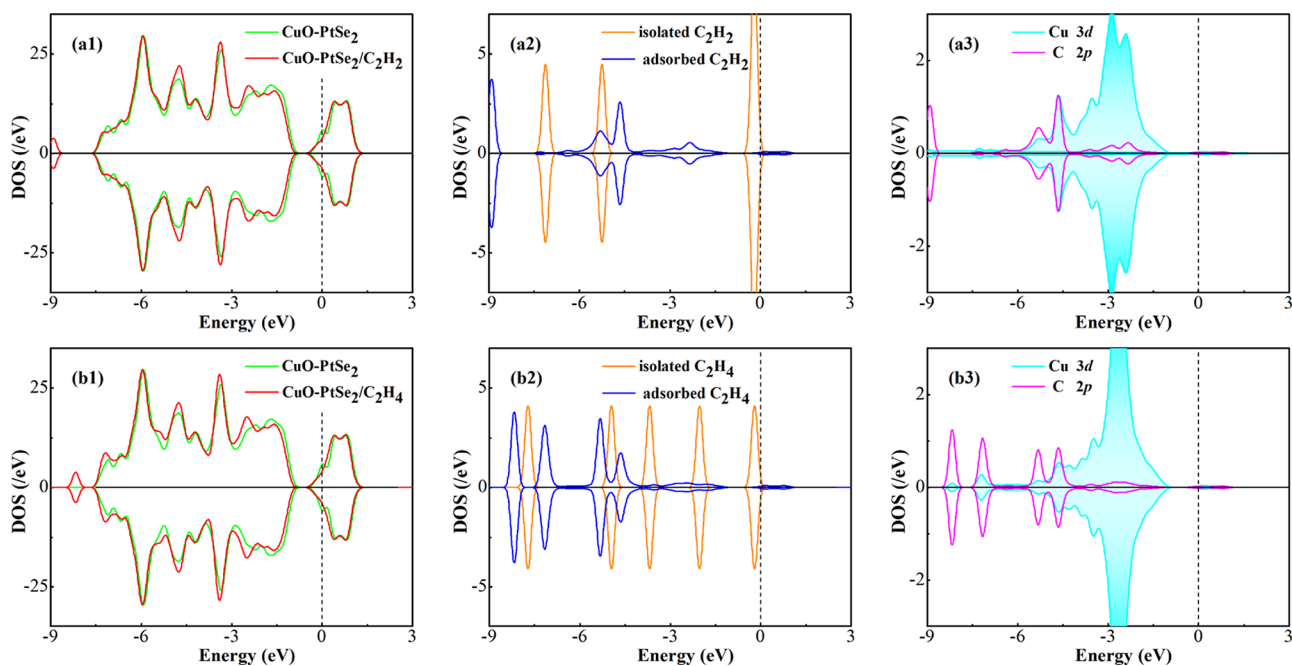
Figure 4. Total, partial, and orbital DOS of (a1−a3) C_2H_2 system and (b1,b2) C_2H_4 system. The sets are the same as those in Figure 2.

C_2H_2 and C_2H_4 systems were obtained and are exhibited in Figure 3. One should note that the CDD here is plotted using the total electron density of the $CuO-PtSe_2$/gas system subtracting the electron densities of the isolated $CuO-PtSe_2$ system and the gas molecule.

For C_2H_2 adsorption on the $CuO-PtSe_2$ monolayer, one can see that the two C atoms of the C_2H_2 molecule are captured by the Cu atom, and the O atom is not involved in such an interaction. The Cu−C bonds are measured to be equally 1.98 Å. The Cu−Se and O−Se bonds are, respectively, prolonged to 2.44 and 1.78 Å, and the Cu−O bond is shortened to be 1.94 Å, which indicates the geometric deformation of the $CuO-PtSe_2$ monolayer caused by C_2H_2 adsorption. Also, we can see that the C_2H_2 molecule undergoes some distortions on the top of the CuO nanoparticle as well, deforming its linear structure instead. The E_{ad} of this system is calculated to be −1.19 eV, which shows the strong binding force between the CuO nanoparticle and the C_2H_2 molecule, especially the newly formed Cu−C bonds.[41] From the Hirshfeld analysis, the CuO nanoparticle is charged by −0.084 e, and the C_2H_2 molecule is charged by 0.040 e. These results reveal that the C_2H_2 molecule in the adsorption donates 0.040 e to the $CuO-PtSe_2$, in which the CuO nanoparticle loses 0.035 e, while the $PtSe_2$ surface accepts 0.075 e. According to the CDD distribution, the Cu−C bonds are embraced with strong electron accumulation, which indicates the strong electron hybridization between the Cu and C atoms that promotes the formations of Cu−C bonds,[42] while the electron depletion is mainly observed on the C_2H_2 molecule and Cu atom, which suggests their electron-donating property.[43]

In the C_2H_4 adsorbed system, it is seen that the O atom of the CuO nanoparticle has no reaction with the C_2H_4 molecule as well, which is similar to that of the C_2H_2 system. It is the Cu atom of the CuO nanoparticle that bonds with the two C atoms of the C_2H_4 molecule, forming two Cu−C bonds, both measured to be 2.03 Å. In the meanwhile, the C_2H_4 molecule in the adsorption experiences some distortion and is not a

plane structure after adsorption. The Ni−Se and O−Se bonds of the $CuO-PtSe_2$ monolayer and the Cu−O bond of the CuO nanoparticle are measured to be 2.44, 1.78 Å, and 1.94 Å, respectively, which indicates the geometric activation in the $CuO-PtSe_2$ monolayer caused by C_2H_4 adsorption.[44] Interestingly, these bond lengths are equal to those in the C_2H_2 system, indicating the comparable adsorption performance of the $CuO-PtSe_2$ monolayer upon these two gas species. The E_{ad} in the C_2H_4 system is obtained as −1.24 eV, slightly more negative than that of the C_2H_2 system. Based on the Hirshfeld analysis, the C_2H_4 molecule is positively charged by 0.011 e, while the CuO nanoparticle is charged by −0.061 e. These findings reveal that the C_2H_4 molecule and the CuO nanoparticle, respectively, lose 0.01 and 0.058 e in the adsorption, resulting in the $PtSe_2$ surface accepting 0.068 e instead. From the CDD, the electron accumulations are surrounded not only on the Cu−C bond, verifying its strong electron hybridization during the new bond formation,[45] but also on the O atom due to its strong electronegativity, similar to that in the C_2H_2 system; on the other hand, the electron depletions are observed on the C_2H_4 molecule, confirming its electron-releasing property, and the Cu atom given its strong electron-donating property in the gas interactions.[46]

As a short summary, the C_2H_2 and C_2H_4 molecules both exhibit an electron-donating property when being adsorbed on the $CuO-PtSe_2$ monolayer, and such gas interactions can be determined to be chemisorption given their negative values, in which their absolute values are larger than the critical value of 0.80 eV.[47]

3.3. DOS Analysis of the gas Systems. Figure 4 presents the DOS of the C_2H_2 and C_2H_4 adsorbed systems to elucidate the electronic properties of the $CuO-PtSe_2$ monolayer upon gas adsorptions. From the total DOS of the isolated and gas adsorbed $CuO-PtSe_2$ systems, one can see that the electronic states of the isolated $CuO-PtSe_2$ monolayer suffer some deformation, especially around the Fermi level. Also, the band gap of the C_2H_2 and C_2H_4 adsorbed systems are obtained as 0.00 eV as well. Besides, there appear several novel states in the

gas adsorbed system compared with those in the isolated CuO−PtSe$_2$ system. These can be attributed to the adsorption of gas species whose DOS states are activated after gas adsorption, therefore deforming the total DOS of the isolated CuO−PtSe$_2$ monolayer accordingly.[48] Such a phenomenon can be observed from the partial DOS of the gas molecule before and after adsorption. It is seen from the DOS that the states of the freestanding gas molecules experience significant deformations in the gas adsorption, and the states are split into several small states, shifting to the regions below the Fermi level. Therefore, it is the activated DOS of the gas species that contributes to the total DOS of the gas adsorbed systems.

From the orbital DOS of the bonded atoms, one can see that the Cu 3d orbital is hybridized with the C 2p orbital of the C$_2$H$_2$ molecule at −7.3, −6.4, −5.3, −4.7, −3.6, −2.9, and −2.4 eV, while it is hybridized with that of the C$_2$H$_4$ molecule at −8.2, −7.1, −5.3, −4.6, −3.6, and −2.7 eV. Besides, there have also been observed some hybridizations at the Fermi level between the Cu and C atoms in two systems, which also contributes largely to the formation of the Cu−C bond and therefore impacts the deformations of the electronic properties of the clean CuO−PtSe$_2$ monolayer. These state hybridizations also verify the strong orbital interaction in the newly formed Cu−C bonds, confirming their strong binding force (Figure 4).

3.4. Gas Sensing Explorations. The deformed electronic property of the CuO−PtSe$_2$ monolayer after gas adsorption accords to its change of electrical conductivity, which can provide the basic sensing mechanism to explore the CuO−PtSe$_2$ monolayer as a resistance-type gas sensor. However, given the zero band gap property of the CuO−PtSe$_2$ monolayer and related gas adsorbed systems, the analysis of the band gap change cannot provide the convincing evidence for its gas sensing performance. Therefore, the charge transfer property is applied to give a clear explanation upon the sensing property of the CuO−PtSe$_2$ monolayer. Also, we use the same way to analyze its enhanced sensing property in comparison with that of the pristine PtSe$_2$ monolayer. The E_{ad} and Q_T for gas adsorptions on the pristine and CuO-decorated PtSe$_2$ monolayer are listed in Table 1.

Table 1. E_{ad} and Q_T for Gas Adsorptions on the Pristine and CuO-Decorated PtSe$_2$ Monolayers

	E_{ad} (eV)	Q_T (e)
PtSe$_2$/C$_2$H$_2$	−0.20	−0.019
PtSe$_2$/C$_2$H$_4$	−0.20	−0.006
CuO−PtSe$_2$/C$_2$H$_2$	−1.19	0.040
CuO−PtSe$_2$/C$_2$H$_4$	−1.24	0.011

For gas adsorptions on the pristine PtSe$_2$ surface, one can see that the Q_T is obtained as −0.019 and −0.006 e in the C$_2$H$_2$ and C$_2$H$_4$ systems, respectively, which indicates the electron-accepting property of the gas species. Our calculations show that the pristine PtSe$_2$ monolayer is a p-type semiconductor, with a closer gap between the valence band and the Fermi level than the gap between the conduction band and the Fermi level. From this aspect, the electron-losing property for the hole-dominated PtSe$_2$ monolayer can cause the increased electrical conductivity. However, given the large band gap of 1.31 eV and the small charge transfer value, one can assume that the increased electrical conductivity would not be quite significant. On the other hand, it has been stated that the adsorption of the CuO nanoparticle results in strong n-type

doping to the PtSe$_2$ monolayer, making the CuO−PtSe$_2$ monolayer an n-type material instead.[49] In that case, the adsorptions of C$_2$H$_2$ and C$_2$H$_4$ with accepted 0.040 and 0.011 e on the CuO−PtSe$_2$ monolayer, respectively, would enhance the electron density of the electron-dominated n-type CuO−PtSe$_2$ monolayer, implying the promoted electrical conductivity of the CuO−PtSe$_2$ monolayer in the C$_2$H$_2$ or C$_2$H$_4$ systems as well.[50] Considering the stronger charge transfer in the CuO−PtSe$_2$/gas systems than in the PtSe$_2$/gas systems, one can infer that the CuO−PtSe$_2$ monolayer can exhibit a stronger sensing performance upon C$_2$H$_2$ and C$_2$H$_4$ detection than the pristine PtSe$_2$ monolayer. In other words, the CuO−PtSe$_2$ monolayer is a promising C$_2$H$_2$ or C$_2$H$_4$ sensor for realizing their detections using the basic sensing mechanism of the enhanced electrical conductivity in the gas atmosphere. However, we should note that the selectivity of these two gas species cannot be realized in their mixed atmosphere, and such an issue may be addressed by imbuing the sensor array with more sensing characteristic for the two gases. Even so, we assume that the detections of either of these two gases, no matter which one, can realize the arc discharge monitoring since they are both the dominant species in such insulation defects. From this aspect, we infer that the CuO−PtSe$_2$ monolayer can be explored as a gas sensor to monitor the arc discharge in an oil-immersed electrical transformer.

Moreover, the recovery time (τ) is calculated to evaluate the reusability of the CuO−PtSe$_2$ monolayer for gas sensing application and compared with that of the pristine PtSe$_2$ monolayer, using the van't Hoff−Arrhenius theory[51] in eq 3

$$\tau = A^{-1}e^{(-E_{ad}/K_B T)} \qquad (3)$$

in which K_B is the Boltzmann constant, with a value of 8.318 × 10^{-3} kJ/(mol·K), A is the attempt frequency, with a value of 10^{16} s^{-1} for UV light,[52] and T is the temperature. Using the equation, the recovery time for the adsorbed C$_2$H$_2$ or C$_2$H$_4$ desorption from the pristine PtSe$_2$ monolayer is calculated to be 2.4 × 10^{-13} s at room temperature, and one can find that such a short time on the sensor's surface cannot allow its detection upon gas molecules. In the meanwhile, the C$_2$H$_2$ and C$_2$H$_4$ desorption times from the CuO−PtSe$_2$ surface are obtained as 1.31 × 10^4 and 9.17 × 10^4 s at room temperature (298 K), respectively, and are obtained as 0.12 and 0.50 s at 398 K, respectively. We can find that the desorption property at 398 K is quite desirable for recycle use of such a sensing material. Therefore, we assume that the CuO−PtSe$_2$ monolayer can be explored as an outstanding room-temperature C$_2$H$_2$ and C$_2$H$_4$ sensor with good recyclability at 398 K,[53] while the pristine PtSe$_2$ monolayer is not suitable for gas sensing exploration.

The work function (WF, φ) is calculated and plotted in Figure 5 to further study the possibility of the CuO−PtSe$_2$ in the Kelvin probe device for the detection of C$_2$H$_2$ for C$_2$H$_4$,[54] which is calculated according to eq 4

$$\varphi = V_{el} - E_f \qquad (4)$$

where V_{el} and E_f represent the electrostatic potential energy far from the material's surface and the Fermi level energy, respectively. From this figure, one could find that the WF of the isolated CuO−PtSe$_2$ monolayer is calculated to be 4.76 eV, which is slightly larger than that of graphene (4.60 eV[55]), suggesting its stronger electron affinity than that of graphene. In the meanwhile, the WFs of the C$_2$H$_2$ and C$_2$H$_4$ systems are calculated to be 4.60 and 4.59 eV, respectively. That is, the
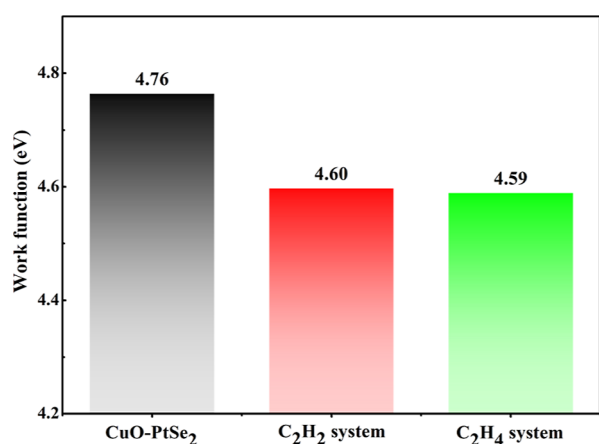
Figure 5. WF of the CuO−PtSe$_2$ monolayer with and without C$_2$H$_2$ and C$_2$H$_4$ adsorbed.

WFs of the CuO−PtSe$_2$ monolayer are decreased obviously after the adsorption of C$_2$H$_2$ and C$_2$H$_4$ molecules, which are about 0.16 eV (3.4%) and 0.17 eV (3.6%), respectively, in comparison with that of the clean CuO−PtSe$_2$ system. Considering these findings, we presume that the CuO−PtSe$_2$ monolayer can exhibit a desirable sensing response upon C$_2$H$_2$ or C$_2$H$_4$ detection based on the change of the WF using the Kelvin probe device, showing admirable suitability for sensor use.[56]

4. CONCLUSIONS

Using the DFT method, we propose the CuO−PtSe$_2$ monolayer as a promising gas sensor for C$_2$H$_2$ and C$_2$H$_4$ in order to realize the DGA in oil-immersed transformers. The main conclusions are as follows:

(i) The adsorption of CuO nanoparticle causes strong n-type doping for the PtSe$_2$ monolayer with a binding force (E_b) of −2.49 eV;

(ii) The CuO−PtSe$_2$ monolayer exhibits strong chemisorption and electron-accepting properties in the two gas systems, with E_{ad} and Q_T obtained as −1.19 eV and 0.040 e for the C$_2$H$_2$ system and as −1.24 eV and 0.011 e for the C$_2$H$_4$ system, respectively.

(iii) The electrical conductivity of the CuO−PtSe$_2$ monolayer would be increased, while the WF would be decreased in the C$_2$H$_2$ or C$_2$H$_4$ atmosphere, showing its potential as a resistance-type or a WF-type gas sensor.

This paper theoretically investigates the sensing potential of PtSe$_2$-based materials for dissolved gases in the transformer oil, which can pave the way for the exploration of novel metal-oxide decorated TMDs for gas sensing application in electrical engineering significantly.

AUTHOR INFORMATION

Corresponding Author

Jianfang Chen − *State Grid Anhui Electric Power Co., Ltd. Maanshan Power Supply Company, Hefei 243011 Anhui, China;* ◉ orcid.org/0000-0002-0167-6200; Email: chenjfcqu@163.com

Authors

Longzhen Wang − *State Grid Anhui Electric Power Co., Ltd. Maanshan Power Supply Company, Hefei 243011 Anhui, China*

Changhong Liu − *State Grid Anhui Electric Power Co., Ltd. Maanshan Power Supply Company, Hefei 243011 Anhui, China*

Min Wei − *State Grid Anhui Electric Power Co., Ltd. Maanshan Power Supply Company, Hefei 243011 Anhui, China*

Xuchu Xu − *State Grid Anhui Electric Power Co., Ltd. Maanshan Power Supply Company, Hefei 243011 Anhui, China*

Complete contact information is available at:
https://pubs.acs.org/10.1021/acsomega.2c06332

Notes

The authors declare no competing financial interest.

ACKNOWLEDGMENTS

REFERENCES

(1) Cui, H.; Zhang, X.; Zhang, G.; Tang, J. Pd-doped MoS2 monolayer: A promising candidate for DGA in transformer oil based on DFT method. *Appl. Surf. Sci.* **2019**, *470*, 1035−1042.

(2) Liao, R.; Zheng, H.; Grzybowski, S.; Yang, L.; Zhang, Y.; Liao, Y. An Integrated Decision-Making Model for Condition Assessment of Power Transformers Using Fuzzy Approach and Evidential Reasoning. *IEEE Trans. Power Delivery* **2011**, *26*, 1111−1118.

(3) Ding, J.; Li, X.; Cao, J.; Sheng, L.; Yin, L.; Xu, X. New sensor for gases dissolved in transformer oil based on solid oxide fuel cell. *Sens. Actuators, B* **2014**, *202*, 232−239.

(4) Cui, H.; Chen, D.; Zhang, Y.; Zhang, X. Dissolved gas analysis in transformer oil using Pd catalyst decorated MoSe2 monolayer: A first-principles theory. *Sustainable Mater. Technol.* **2019**, *20*, No. e00094.

(5) He, X.; Gui, Y.; Xie, J.; Liu, X.; Wang, Q.; Tang, C. A DFT study of dissolved gas (C2H2, H2, CH4) detection in oil on CuO-modified BNNT. *Appl. Surf. Sci.* **2020**, *500*, 144030.

(6) Yang, F.; Jung, D.; Penner, R. M. Trace Detection of Dissolved Hydrogen Gas in Oil Using a Palladium Nanowire Array. *Anal. Chem.* **2011**, *83*, 9472−9477.

(7) Mak, T.; Westerwaal, R. J.; Slaman, M.; Schreuders, H.; van Vugt, A. W. V.; Victoria, M.; Boelsma, C.; Dam, B. Optical fiber sensor for the continuous monitoring of hydrogen in oil. *Sens. Actuators, B* **2014**, *190*, 982−989.

(8) Samsudin, M. R.; Shee, Y. G.; Mahamd Adikan, F. R.; Dahari, M. Fiber Bragg Gratings (FBG) Hydrogen Sensor for Transformer Oil Degradation Monitoring. *IEEE Sens. J.* **2016**, *16*, 2993.

(9) Ma, G. M.; Li, C. R.; Luo, Y. T.; Mu, R. D.; Wang, L. High sensitive and reliable fiber Bragg grating hydrogen sensor for fault detection of power transformer. *Sens. Actuators, B* **2012**, *169*, 195−198.

(10) Singh, S.; Bandyopadhyay, M. N. Dissolved gas analysis technique for incipient fault diagnosis in power transformers: A bibliographic survey. *IEEE Electr. Insul. Mag.* **2010**, *26*, 41−46.

(11) Zhang, G.; Zhang, X.; Cheng, H.; Tang, J. Ladder-wise calculation method for z-coordinate of transformer PD source based on planar layout UHF antenna sensors. *IEEJ Trans. Electr. Electron. Eng.* **2020**, *15*, 340.

(12) Benounis, M.; Aka-Ngnui, T.; Jaffrezic, N.; Dutasta, J. P. NIR and optical fiber sensor for gases detection produced by transformation oil degradation. *Sens. Actuators, A* **2008**, *141*, 76−83.

(13) Fan, J.; Wang, F.; Sun, Q.; Ye, H.; Jiang, Q. Application of Polycrystalline SnO2 Sensor Chromatographic System to Detect Dissolved Gases in Transformer Oil. *Sens. Actuators, B* **2018**, *267*, 636.

(14) Kazemi, A.; Rodner, M.; Fadavieslam, M. R.; Kaushik, P. D.; Ivanov, I. G.; Eriksson, J.; Syväjärvi, M.; Yakimova, R.; Yazdi, G. R.

The effect of Cl- and N-doped MoS2 and WS2 coated on epitaxial graphene in gas-sensing applications. *Surf. Interfaces* 2021, 25, 101200.

(15) Li, F.; Asadi, H. DFT study of the effect of platinum on the H2 gas sensing performance of ZnO nanotube: explaining the experimental observations. *J. Mol. Liq.* 2020, 309, 113139.

(16) Sun, X.; Yang, Q.; Meng, R.; Tan, C.; Liang, Q.; Jiang, J.; Ye, H.; Chen, X. Adsorption of gas molecules on graphene-like InN monolayer: A first-principle study. *Appl. Surf. Sci.* 2017, 404, 291−299.

(17) Zhao, S.; Xue, J.; Kang, K. Gas adsorption on MoS2 monolayer from first-principles calculations. *Chem. Phys. Lett.* 2014, 595−596, 35−42.

(18) Kronberg, R.; Hakala, M.; Holmberg, N.; Laasonen, K. Hydrogen adsorption on MoS2-surfaces: a DFT study on preferential sites and the effect of sulfur and hydrogen coverage. *Phys. Chem. Chem. Phys.* 2017, 19, 16231.

(19) Chia, X.; Adriano, A.; Lazar, P.; Sofer, Z.; Luxa, J.; Pumera, M. Layered platinum dichalcogenides (PtS2, PtSe2, and PtTe2) electrocatalysis: monotonic dependence on the chalcogen size. *Adv. Funct. Mater.* 2016, 26, 4306−4318.

(20) Li, P.; Hong, Q.; Wu, T.; Cui, H. SOF2 sensing by Rh-doped PtS2 monolayer for early diagnosis of partial discharge in the SF6 insulation device. *Mol. Phys.* 2021, 119, No. e1919774.

(21) Chen, D.; Zhang, X.; Tang, J.; Cui, Z.; Cui, H.; Pi, S. Theoretical study of monolayer PtSe2 as outstanding gas sensor to detect SF6 decompositions. *IEEE Electron Device Lett.* 2018, 39, 1405−1408.

(22) Li, D.; Rao, X.; Zhang, L.; Zhang, Y.; Ma, S.; Chen, L.; Yu, Z. First-Principle Insight into the Ru-Doped PtSe2 Monolayer for Detection of H2 and C2H2 in Transformer Oil. *ACS Omega* 2020, 5, 31872−31879.

(23) Sajjad, M.; Montes, E.; Singh, N.; Schwingenschlögl, U. Superior Gas Sensing Properties of Monolayer PtSe2. *Adv. Mater. Interfaces* 2017, 4, 1600911.

(24) Kamal, T. High performance NiO decorated graphene as a potential H2 gas sensor. *J. Alloys Compd.* 2017, 729, 1058−1063.

(25) Chen, Y.; Gui, Y.; Chen, X. Adsorption and gas-sensing properties of C2H4, CH4, H2, H2O on metal oxides (CuO, NiO) modified SnS2 monolayer: A DFT study. *Results Phys.* 2021, 28, 104680.

(26) Kadioglu, Y.; Gökoğlu, G.; Üzengi Aktürk, O. Molecular adsorption properties of CO and H2O on Au-, Cu-, and AuxCuy-doped MoS2 monolayer. *Appl. Surf. Sci.* 2017, 425, 246−253.

(27) Gao, M.; Lyalin, A.; Taketsugu, T. Oxygen activation and dissociation on h-BN supported Au atoms. *Int. J. Quantum Chem.* 2013, 113, 443−452.

(28) Cui, H.; Jia, P.; Peng, X.; Hu, X. Geometric, Electronic and Optical Properties of Pt-Doped C3N Monolayer Upon NOx Adsorption: A DFT Study. *IEEE Sens. J.* 2021, 21, 3602−3608.

(29) Cui, H.; Jia, P.; Peng, X. Adsorption of SO2 and NO2 molecule on intrinsic and Pd-doped HfSe2 monolayer: A first-principles study. *Appl. Surf. Sci.* 2020, 513, 145863.

(30) Zhang, D.; Li, Q.; Li, P.; Pang, M.; Luo, Y. Fabrication of Pd-decorated MoSe 2 nanoflowers and density functional theory simulation toward ammonia sensing. *IEEE Electron Device Lett.* 2019, 40, 616−619.

(31) Tkatchenko, A.; DiStasio, R. A., Jr.; Head-Gordon, M.; Scheffler, M. Dispersion-corrected Møller-Plesset second-order perturbation theory. *J. Chem. Phys.* 2009, 131, 094106.

(32) Cui, H.; Yan, C.; Jia, P.; Cao, W. Adsorption and sensing behaviors of SF6 decomposed species on Ni-doped C3N monolayer: A first-principles study. *Appl. Surf. Sci.* 2020, 512, 145759.

(33) Ma, D.; Wang, Y.; Liu, L.; Jia, Y. Electrocatalytic nitrogen reduction on the transition-metal dimer anchored N-doped graphene: performance prediction and synergetic effect. *Phys. Chem. Chem. Phys.* 2021, 23, 4018−4029.

(34) Lin, S.; Ye, X.; Johnson, R. S.; Guo, H. First-Principles Investigations of Metal (Cu, Ag, Au, Pt, Rh, Pd, Fe, Co, and Ir) Doped Hexagonal Boron Nitride Nanosheets: Stability and Catalysis of CO Oxidation. *J. Phys. Chem. C* 2013, 117, 17319−17326.

(35) Deng, S.; Li, L.; Zhang, Y. Strain Modulated Electronic, Mechanical, and Optical Properties of the Monolayer PdS2, PdSe2, and PtSe2 for Tunable Devices. *ACS Appl. Nano Mater.* 2018, 1, 1932−1939.

(36) Murphy, L. R.; Meek, T. L.; Allred, A. L.; Allen, L. C. Evaluation and test of pauling's electronegativity scale. *J. Phys. Chem. A* 2000, 104, 5867−5871.

(37) Rauch, C.; Tuomisto, F.; VilaltaClemente, A.; Lacroix, B.; Ruterana, P.; Kraeusel, S.; Hourahine, B.; Schaff, W. J. Defect evolution and interplay in n-type InN. *Appl. Phys. Lett.* 2012, 100, 091907.

(38) Duan, X. M.; Stampfl, C. Nitrogen vacancies in InN: Vacancy clustering and metallic bonding from first principles. *Phys. Rev. B: Condens. Matter Mater. Phys.* 2008, 77, 115207.

(39) Cui, H.; Zhang, X.; Li, Y.; Chen, D.; Zhang, Y. First-principles insight into Ni-doped InN monolayer as a noxious gases scavenger. *Appl. Surf. Sci.* 2019, 494, 859−866.

(40) Kou, L.; Frauenheim, T.; Chen, C. Phosphorene as a Superior Gas Sensor: Selective Adsorption and Distinct I−V Response. *J. Phys. Chem. Lett.* 2014, 5, 2675−2681.

(41) Zhang, X.; Wang, J.; Chen, D.; Liu, L. The adsorption performance of harmful gas on Cu doped WS2: A First-principle study. *Mater. Today Commun.* 2021, 28, 102488.

(42) Yang, A.; Wang, D.; Wang, X.; Zhang, D.; Koratkar, N.; Rong, M. Recent advances in phosphorene as a sensing material. *Nano Today* 2018, 20, 13−32.

(43) Ju, W.; Li, T.; Su, X.; Li, H.; Li, X.; Ma, D. Au cluster adsorption on perfect and defective MoS2 monolayers: structural and electronic properties. *Phys. Chem. Chem. Phys.* 2017, 19, 20735.

(44) Fan, Y.; Zhang, J.; Qiu, Y.; Zhu, J.; Zhang, Y.; Hu, G. A DFT study of transition metal (Fe, Co, Ni, Cu, Ag, Au, Rh, Pd, Pt and Ir)-embedded monolayer MoS2 for gas adsorption. *Comput. Mater. Sci.* 2017, 138, 255−266.

(45) Zhou, Q.; Zhang, G.; Tian, S.; Zhang, X. First-Principles Insight into Pd-Doped ZnO Monolayers as a Promising Scavenger for Dissolved Gas Analysis in Transformer Oil. *ACS Omega* 2020, 5, 17801−17807.

(46) Tanvir, N. B.; Yurchenko, O.; Laubender, E.; Urban, G. Investigation of low temperature effects on work function based CO2 gas sensing of nanoparticulate CuO films. *Sens. Actuators, B* 2017, 247, 968−974.

(47) Huang, J.; Chu, J.; Wang, Z.; Zhang, J.; Yang, A.; Li, X.; Gao, C.; Huang, H.; Wang, X.; Cheng, Y.; Rong, M. Chemisorption of NO2 to MoS2 Nanostructures and its Effects for MoS2 Sensors. *ChemNanoMat* 2019, 5, 1123−1130.

(48) Zhao, G.; Li, M. Ni-doped MoS2 biosensor: a promising candidate for early diagnosis of lung cancer by exhaled breathe analysis. *Appl. Phys. A* 2018, 124, 751.

(49) Xia, H.; Lu, Z. Y.; Li, T. X.; Parkinson, P.; Liao, Z. M.; Liu, F. H.; Lu, W.; Hu, W. D.; Chen, P. P.; Xu, H. Y.; Zou, J.; Jagadish, C. Distinct photocurrent response of individual GaAs nanowires induced by n-type doping. *Acs Nano* 2012, 6, 6005−6013.

(50) Zhang, D.; Jiang, C.; Wu, J. Layer-by-layer assembled In2O3 nanocubes/flower-like MoS2 nanofilm for room temperature formaldehyde sensing. *Sens. Actuators, B* 2018, 273, 176−184.

(51) Zhang, Y.-H.; Chen, Y.-B.; Zhou, K.-G.; Liu, C.-H.; Zeng, Z.; Zhang, H.-L.; Peng, Y. Improving gas sensing properties of graphene by introducing dopants and defects: a first-principles study. *Nanotechnology* 2009, 20, 185504.

(52) Vadalkar, S.; Chodvadiya, D.; Som, N. N.; Vyas, K. N.; Jha, P. K.; Chakraborty, B. An Ab-initio Study of the C18 nanocluster for Hazardous Gas Sensor Application. *ChemistrySelect* 2022, 7, No. e202103874.

(53) Rajput, K.; Kumar, V.; Roy, D. R. Heterobilayer CaS/CaSe: A promising sensor for environmental toxic NO2 gas with high selectivity and sensitivity. *Appl. Surf. Sci.* 2020, 528, 146996.

(54) Li, F.; Gao, X.; Wang, R.; Zhang, T.; Lu, G. Study on TiO2-SnO2 core-shell heterostructure nanofibers with different work function and its application in gas sensor. *Sens. Actuators, B* **2017**, *248*, 812−819.

(55) Yu, Y. J.; Zhao, Y.; Ryu, S.; Brus, L. E.; Kim, K. S.; Kim, P. Tuning the graphene work function by electric field effect. *Nano Lett.* **2009**, *9*, 3430−3434.

(56) Patel, S.; Patel, P.; Chodvadiya, D.; Som, N. N.; Jha, P. K. Adsorption performance of C12, B6N6 and Al6N6 nanoclusters towards hazardous gas molecules: A DFT investigation for gas sensing and removal application. *J. Mol. Liq.* **2022**, *352*, 118702.